TECHNISCHE MECHANIK, Band ??, Heft ?, (2004), ??– ??
Manuskripteingang: 4 April 2004

Inextensional Packaging of Thin Shell Slit Reflectors

B. Tibbalds, S.D. Guest and S. Pellegrino

Carbon-fibre-reinforced-plastic reflector antennas based on a thin shell that is folded elastically have been recently developed; this paper presents a new concept for packaging reflectors of this type. The idea is to cut the surface into 6-8 petals along curved lines, whose shape is such that in the packaged configuration the petals wrap around a central part. During deployment, they open out and unwrap, driven by the energy stored during folding. Analytical expressions are derived for the stresses induced by inextensional elastic folding of a doubly-curved shell. A simple, approximate method for analysing the packaging scheme is introduced, and its predictions are used to set up an optimization scheme that determines the cutting pattern required to achieve optimal packaging of the reflector, for a given yield stress and elastic modulus of the material. For a dish with diameter of 0.9 m an optimised cutting pattern is determined, and then a detailed finite-element analysis and an experimental verification of the curvatures induced by packaging are carried out. These results confirm that these predictions from the approximate analysis are accurate and conservative. A reduction in diameter of 3 is achieved for this particular dish.

1 Introduction

New challenges have recently emerged in the field of deployable spacecraft reflectors, as there is a growing demand for reflectors with aperture diameters of 5 to 10 m, whereas the largest launch vehicle continue to have diameters of around 4.5 m, and cheaper launchers have significantly smaller diameters. One option is to use furlable mesh reflectors, which however are limited in the accuracy of the reflective surface that can be achieved. Higher accuracy requires a continuous reflective surface, whose traditional implementation has been in the form of a segmented rigid surface whose parts are connected by hinges, but deployable reflectors of this kind are expensive, complex, and heavy.

A mould-breaking innovation was the development of carbon-fibre-reinforced-plastic antennas with a flexible reflective surface (Robinson, 1992). These antennas are elastically folded about a diameter, like "taco shells"; an example is shown in Figure 1. The folding scheme is simple and effective, however it is feasible only if there is space to stow a long and narrow object.

The present paper explores an alternative, more compact packaging scheme that also involves folding elastically a large dish. Figure 2 shows a photograph of a small scale model, folded according to the new scheme. It resembles a flower, like many other solid surface reflectors in their packaged state (Mikulas and Thomson, 1994). This particular

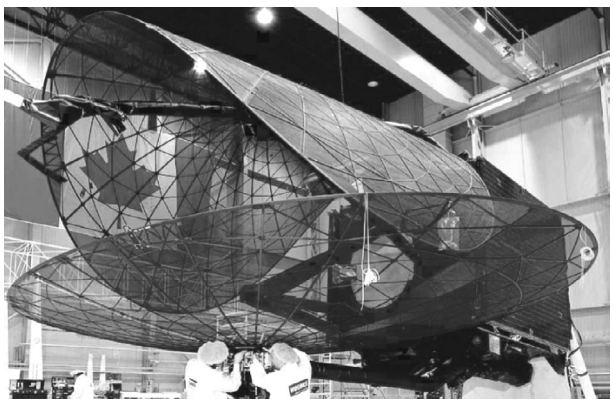

Figure 1: Two "taco shell" reflectors for MSAT, one folded and one deployed.

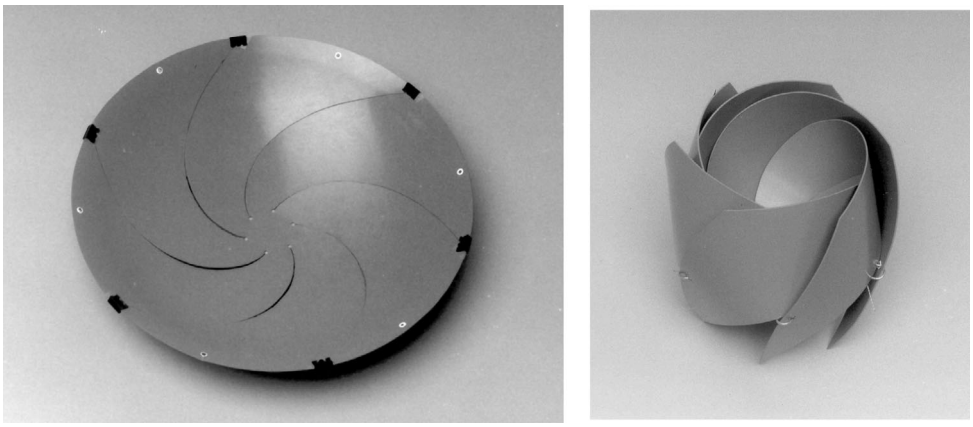

Figure 2: Small scale model, deployed and packaged.

scheme consists of 6 *petals* that fit together in a cylindrical manner about a central hub. During deployment, the petals open out and unwrap, and then their edges are pulled together by springs or other devices. This folding scheme is inherited from a concept for rigid-surface reflectors proposed by Guest and Pellegrino (1996), which makes use of similarly wrapped, segmented petals consisting of rigid panels connected by revolute joints. Six coupling bars, driven by 6 geared motors, connect adjacent petals, and synchronously deploy the whole structure. In the present approach the solid panels and hinges have been replaced by elastically deformable petals.

This paper is divided into six sections. Following this Introduction, Section 2 derives approximate analytical expressions for the stresses induced by *inextensional* elastic folding of a doubly-curved shell. Then, Sections 3 and 4 present the new folding concept, first in a simplified form whose geometrical details are easier to understand, and then in full. A scheme for optimising the size of the packaged reflector, subject to the maximum stress being lower than a prescribed limit, is presented. Section 5 presents a finite-element analysis and experimental verification of the optimised folding scheme for a dish with a diameter of 0.9 m, divided into 6 petals. A discussion concludes the paper.

2 Curvature Limits

This section presents an approximate way of estimating the stresses generated by elastically folding an axisymmetric parabolic reflector of aperture diameter D and focal length F. It is assumed that the reflector consists of a thin shell of uniform thickness t, made of homogeneous, linear-elastic and isotropic material of Young's Modulus E and Poisson's ratio ν.

The local curvature of a paraboloidal surface varies with the distance from the apex. However, here for simplicity it will be approximated by a spherical cap of radius r which coincides with the paraboloid both at the apex and at the edge, as shown in Figure 3. The following relationships can be derived between F, D and the radius of the sphere, r, and the angle subtended by the spherical cap, θ

$$r = 2F + D^2/32F \tag{1}$$

$$\theta = \sin^{-1} \frac{D/16F}{(D/16F)^2 + 0.25} \tag{2}$$

From Figure 3, $L = r\theta$.

Calladine (1983) discusses the geometry of distortion of curved surfaces. If a shell distorts in pure bending, i.e. without stretching, then the Gaussian curvature, K, which is the product of the principal curvatures at any point of the surface, remains constant. Now, the Gaussian curvature of the undeformed reflector, i.e. the spherical cap, is

$$K = 1/r^2 \tag{3}$$

Consider a sector of a paraboloid, obtained by intersecting the surface with two radial planes. A sector is a simple version of one of the petals shown in Figure 2. Figure 4 shows a way of packaging this sector, by wrapping it N

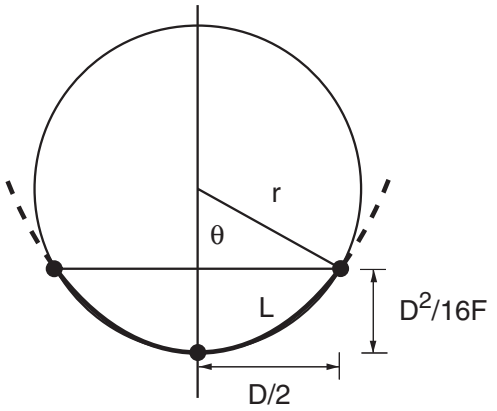

Figure 3: Spherical approximation of a paraboloid.

times around an imaginary cylinder of radius R, where

$$R = L/2N\pi \tag{4}$$

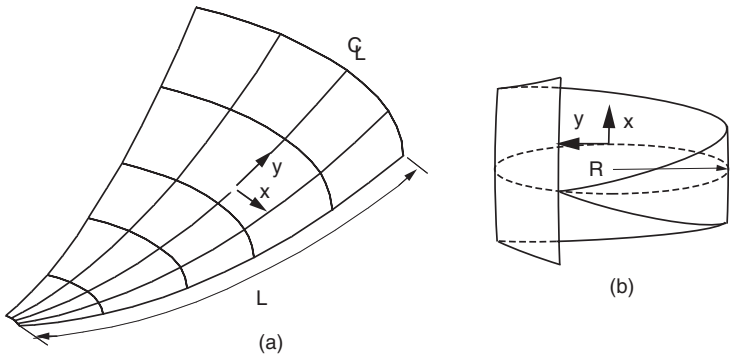

Figure 4: Elastic wrapping of sector of paraboloid, for $N = 1.0$.

It is assumed that the Gaussian curvature remains unchanged during wrapping. Focussing on the centre-line of the sector, where the principal directions of curvature are x, y, both before and after deformation, the principal curvatures are $1/R'$ and $1/R$, respectively. Since the product of these curvatures is equal to K, we can combine equations (3)-(4) to obtain

$$R' = \frac{1}{RK} = \frac{2N\pi r^2}{L} \tag{5}$$

Hence, the elastic curvature changes are

$$\kappa_x = \frac{1}{R'} - \frac{1}{r} \tag{6}$$

$$\kappa_y = \frac{1}{R} - \frac{1}{r} \tag{7}$$

Applying Hooke's Law, and since the mid-plane stresses are zero because the deformation is inextensional, we determine the maximum and minimum principal stresses in the shell from

$$\sigma_x = \pm\frac{E}{1-\nu^2}\left(\kappa_x + \nu\kappa_y\right)\frac{t}{2} \tag{8}$$

$$\sigma_y = \pm\frac{E}{1-\nu^2}\left(\kappa_y + \nu\kappa_x\right)\frac{t}{2} \tag{9}$$

The Von Mises failure criterion, if applicable, may be used to determine the factor of safety against material yielding.

t (mm)	N	R (mm)
0.5	3.9	10.3
1.0	2.0	19.8
1.5	1.4	28.7
2.0	1.1	37.0
2.5	0.9	44.7
3.0	0.8	52.0
4.0	0.6	65.5

Table 1: Minimum radius of folding for Vivak shells with $D = 0.5$ m and $F/D = 0.3$.

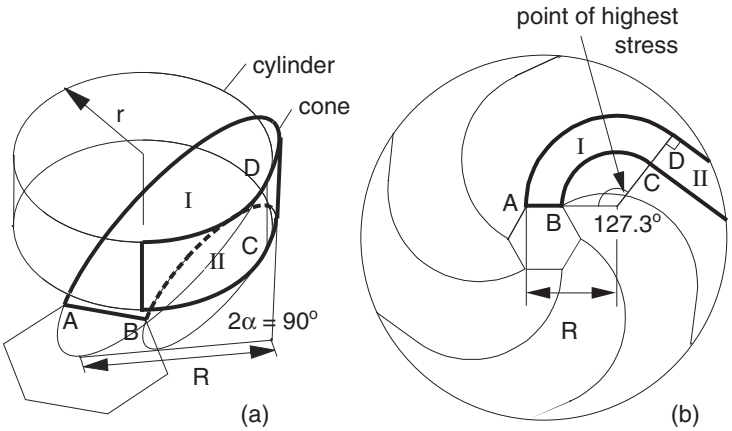

Figure 5: Folding concept.

hence, setting $\sigma_z = 0$

$$\sigma_x^2 - \sigma_x \sigma_y + \sigma_y^2 = Y^2 \tag{10}$$

For example, the dish shown in Figure 2 is made from a low-cost thermoplastic called Vivak, the stress-strain relationship of which is practically linear up to strains of 1.7%. The yield stress of Vivak is $\sigma_y \approx 40$ N/mm^2, its Young's modulus is 1700 N/mm^2, and its Poisson's ratio is 0.4. Applying equations (1)-(10) to a Vivak dish of thickness t with $D = 0.5$ m and $F/D = 0.3$, we have calculated the number of wraps round the cylinder, N, to cause first yield of the shell and the corresponding radius of curvature R at yield. These values are given in Table 1 for different values of t.

3 Folding Concept

The next step is to develop an efficient packaging scheme that involves sub-dividing a thin-shell reflector into a series of petals, which are required only to bend when the reflector is packaged. A way of doing this is to work out a cutting pattern for the edges of the petals, such that longitudinal bending of each petal results in the petals becoming wrapped around the hub. In this analysis the petals can be modelled as flat plates, as their initial curvature is very much smaller than the elastic curvatures associated with the folding process.

In the rigid surface deployable reflector that inspired our folding scheme (Guest and Pellegrino, 1996) each segmented petal turns through 90° as close to the hub as possible, and then wraps around a cylinder. The radius of this cylinder is equal to the hub radius plus the size of the region over which the petal turns through 90°. The simplest shape for this transition region is a cone that is tangent both to the hub and to the cylinder, Figure 5(a). The corresponding cutting pattern consists of a circular arc plus a straight line, Figure 5(b).

There is only one cone that includes an angle $2\alpha = 90^\circ$: the diameter of its base circle is $\sqrt{2}R$, and the angle subtended by its flattened surface is $\sqrt{2}\pi$ rad $= 254.6^\circ$. Only half of this cone is required in the cutting pattern of Figure 5, hence the angle subtended by the cutting pattern for part I of the petal is 127.3°.

Note that, for this packaging scheme to work well, the axis of the cylinder should pass through the centre of the hub, so that all of the petals wrap around the same cylinder, without interference. This does not happen for the present simple version of the folding scheme but will be avoided by introducing a geometric constraint, later on.

3.1 Maximum stress

It is important to examine the stresses in the conical region. The principal curvatures at a point of a cone that is at a distance s from the apex, are $(\cot\alpha)/s$ and 0. Here, $\alpha = 45^\circ$ and hence, if an initially flat petal is rolled into a cone, its elastic curvatures are

$$\kappa_x = 1/s \tag{11}$$
$$\kappa_y = 0 \tag{12}$$

Substituting the above expressions into equations (8)-(9), one finds that the peak stress components are

$$\sigma_x = \pm\frac{E}{1-\nu^2}\frac{t}{2s} \tag{13}$$
$$\sigma_y = \pm\nu\frac{E}{1-\nu^2}\frac{t}{2s} \tag{14}$$

These values, and hence the corresponding von Mises stress are highest when s is smallest. Therefore, when the petal is folded, yielding would occur first at the point that is nearest to the apex of the cone, see Figure 5(b).

4 Packaging Scheme

The folding concept described above is a good way of gaining a geometrical understanding of our packaging scheme, which is a natural evolution of the cone-cylinder idea. The main problems with this simple folding concept are, first, that the petals wrap around a cylinder too soon, which results in interference between the petals and, second, that the part of the cone that is furthest away from the hub is subject to high stresses. To remove these limitations we need to introduce a more general folding scheme.

Consider wrapping each petal around many cones, the apex of which moves further and further away, and eventually around a cylinder. The position of this cylinder can be varied by varying the curvature of the cones. In addition, the apex of the longer cones will move further away from the petal, and hence the stress induced by bending the petal around longer cones is correspondingly reduced.

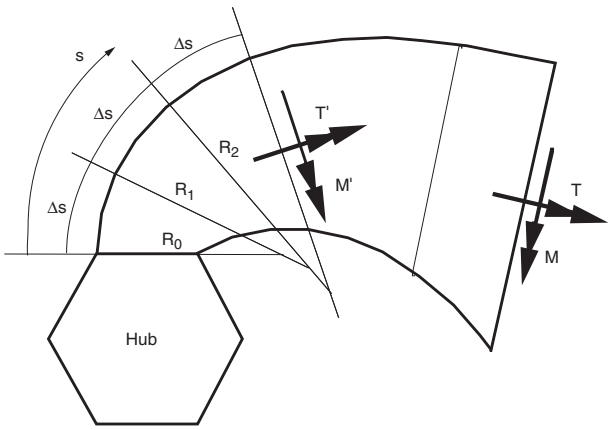

Figure 6: Cutting pattern for cones of increasing height.

Figure 6 illustrates how the sectors that make up the cones may be fitted together on a flat pattern. The radius of curvature of each arc forming the cutting pattern is defined as a function of the distance, s, along the line. Sufficient accuracy is achieved by setting $\Delta s = D/100$.

As a cone with an infinitely high apex is a cylinder, a simple scheme where the radius of arc curvature starts at an initial value, R_0, and then becomes infinite at a specified distance, s_0, is obtained for

$$R = R_0 s_0^n/(s_0 - s)^n \quad \text{for} \quad 0 \le s \le s_0 \tag{15}$$

$$R = \infty \quad \text{for} \quad s_0 \le s \tag{16}$$

Here, R_0, s_0, and n are the three parameters that control the cutting pattern, which is shown in Figure 6 for $n = 1$. The cut begins with a high curvature that gradually decreases. At the line marking the transition from the curved to the straight line the curvature becomes zero.

Although equations (15)-(16) fully define the cutting pattern for a circular thin plate, i.e. for the two-dimensional projection of our reflector, they do not provide enough information on the amount of curvature that should be imparted to each petal. In other words, the height of each cone is R, but the radius of its base circle is not yet known.

An additional equation is obtained by considering the elastic deformation of the petal when it is subject to a bending moment, M, and a twisting moment, T, at the rim, as shown in Figure 6. These moments can be resolved to find the bending moment M' at any cross-section of the petal. Then, modelling the petal as a beam of variable cross-section, its curvature at the chosen cross-section is calculated from

$$\kappa = 12M'/ELt^3 \tag{17}$$

where L is the width of the petal, and t its thickness.

With this, we are ready to study the geometry of a small element of petal, $ABCD$, that is wrapped on a cone, as shown in Figure 7. One side of this patch, AB, is determined by the position of the previous patch, and also the radius R is known from equation (15).

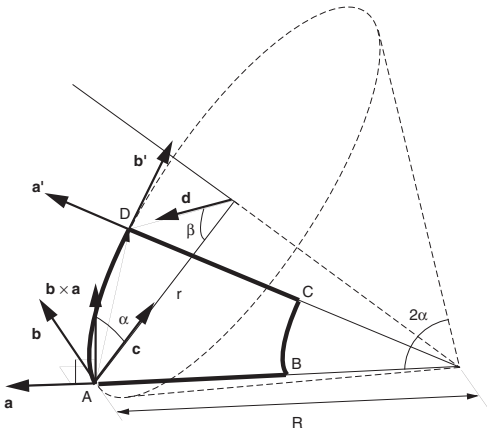

Figure 7: Analysis of conical surface element.

We define the unit vectors $\mathbf{a} = (A - B)/\|AB\|$ and $\mathbf{b}$ tangent to the edge of the cone at A. Analogous vectors are defined at D. The radius of the base circle of the cone is $r = 1/\kappa$, with κ given by equation (17). Hence

$$\alpha = \sin^{-1}(r/R) \tag{18}$$

Since the arc-length AD is equal to Δs,

$$\beta = \Delta s/r \tag{19}$$

Then, simple vector analysis yields

$$\mathbf{c} = \mathbf{b} \times \mathbf{a} \cos\alpha - \mathbf{a} \sin\alpha \tag{20}$$

$$\mathbf{d} = r(\mathbf{b} \sin\beta - \mathbf{c} \cos\beta) \tag{21}$$

$$D - A = r\mathbf{c} + \mathbf{d} \tag{22}$$

$$\mathbf{a}' = \frac{(D-A)\times\mathbf{d}}{\|(D-A)\times\mathbf{d}\|} \tag{23}$$

$$\mathbf{b}' = \frac{\mathbf{d}\times\mathbf{a}'}{\|\mathbf{d}\times\mathbf{a}'\|} \tag{24}$$

Finally, the length of DC can be calculated from the flat pattern, and then C can be found by moving by this distance along $\mathbf{a}'$, from D.

4.1 Computational Procedure

The calculation of a trial packaging scheme for a reflector of diameter D consists of the following steps.

- Definition of the parameters R_0, s_0, n in equations (15)-(16), and of the edge moments M, T, as well as the diameter of the hub, d, and the number of petals.
- Calculation of the co-ordinates of points spaced by $\Delta s = D/100$ on a cutting line that starts at one corner of the hub, using equations (15)-(16).
- Rotation of this line through 360° divided by the number of petals.
- Computation of the deformed shape of the petal using the vector technique described above, by considering a series of conical patches of width Δs.
- Check for interference between neighbouring petals.
- Determination of the maximum stress in the petal by using equations (13)-(14) on each conical patch, and considering the point nearest to the apex of each cone.
- Calculation of the *packaging ratio*, i.e. the distance between the centre point on the transition line between cone and cylinder, divided by the hub radius. The rest of the petal is not considered in this calculation, because it can easily be wrapped around the hub region.

The above procedure was built into an optimization routine by Hooke and Jeeves (1961), which is well suited for constrained optimization problems. This routine looks for the minimum value of (packaging ratio)$^{-1}$ on a multi-dimensional surface implicitly defined by the above computational procedure, subject to the interference and stress constraints that have been discussed.

Initial tests of the optimization routine revealed that this multi-dimensional surface is very complex and uneven. Consequently, there are some relative minima which may be picked up before the global minimum is found. Altering the start parameters is one way of getting round this, so the routine is given a variety of approaches.

The best results were obtained by first using the optimization routine to minimise the angle between the vertical and the line on the petal that marks the final cone-cylinder transition, starting from the undeformed state. In this way the optimization of the diameter packaging ratio starts when the outer region of the petal is already in a nearly vertical plane. It was found that the ratio between aperture and hub diameter, D/d, is an important parameter for the optimization process. Significantly better results were obtained by controlling the value of this parameter. Finally, it was decided to include the twisting deformation of the petal in the analysis, as this produced a small but significant difference in the deformed shape of the petal.

A series of results obtained from this optimization approach for a reflector with $D = 0.5$ m, made of 1.5 mm thick Vivak, are listed in Table 2. The reflector with 5 petals does not work well; its packaging ratio is the worst, and its design —which is limited by the yield stress of the material— does not have the petals wrapping cylindrically around the hub. In addition, the petals become quite wide at the edge, and it is likely that double-curvature effects would limit the validity of our analysis.

Note that the maximum stress decreases as the number of petals increases, whereas the packaging ratio remains relatively constant. The reflectors with 7 and 8 petals appear to package no more efficiently than the reflector with 6 petals. Although these designs are not limited by the maximum stress, they clearly are limited by the geometrical

Number of Petals	5	6	7	8
s_0 (mm)	317.5	300.0	276.0	242.9
R_0 (mm)	102.6	100.0	94.6	111.0
n	0.71	0.62	0.51	0.24
D/d	8.70	8.20	9.36	8.18
M (Nmm)	200.9	160.2	110.0	103.2
T (Nmm)	17.6	20.1	63.0	71.4
σ_{max} (N/mm^2)	39.9	33.5	29.6	20.9
Packing ratio	1.97	2.15	2.01	2.07

Table 2: Optimised packaging schemes.

constraint imposed by interference between the petals. In fact, experiments with small scale models showed that the packaging ratios listed in the table are slightly misleading, because the outer part of each petal can be wrapped much more efficiently if only a small contact force with neighbouring petals is permitted.

In short, the patterns have been optimised to their limit, constrained by the geometry or maximum stress near to the hub. However, improvements can be made by extending the cutting pattern by means of straight lines. The new sections of petal can then be wrapped very efficiently around the hub, which results in a significant improvement in the diameter packaging ratio.

5 Finite Element Verification and Experiment

Although Table 2 would seem to favour reflectors with 7 or 8 petals, due to the lower stresses involved, concerns over the stress concentration in the small hub area of these reflectors led to the choice of a 6-petal reflector to demonstrate the new folding concept. A 2 mm Vivak sheet was heated and drop-formed using a mould. This produced a paraboloidal dish with diameter $D = 0.9$ m and $F/D = 0.4$.

In calculating the cutting pattern, the maximum stress allowed was set at 60% of the yield stress, to avoid excessive creep deformation of the model in the packaged configuration. The optimization process outlined in the previous section produced the parameters listed in Table 3, and the cutting pattern shown in Figure 8. Figure 9 shows the predicted geometry of this dish. The plan view shows that the outer region of the petals can be pulled in more tightly, to achieve a packaging ratio of 3.0.

D	900 mm
s_0	435.1 mm
R_0	139.0 mm
n	0.62
D/d	10.48
M	499.7 Nmm
T	211.2 Nmm
σ_{max}	22.7 N/mm^2
Packing ratio	3.0 (adjusted)

Table 3: Design parameters for experimental model.

At this point, a finite element analysis of a single petal of the curved reflector, cut according to the pattern shown in Figure 8, was carried out. A uniformly graded mesh of linear-strain quadrilateral elements was set up in the ABAQUS (2002) package and, after some preliminary studies, it was found that the best way of achieving convergence was to simulate the folding process by moving the boundary conditions applied to the shell. From the boundary reactions one can work out the force/couple required for folding.

This analysis showed that the maximum von Mises stress, near the edge of the petal that is folded below the hub, occurs near point B in Figure 8. Its value was about 20% lower than predicted by our approximate analysis. The probable reason for this is that, due to its initial curvature, the petal tends to move above the hub as it is wrapped, thus reducing the required curvature change.

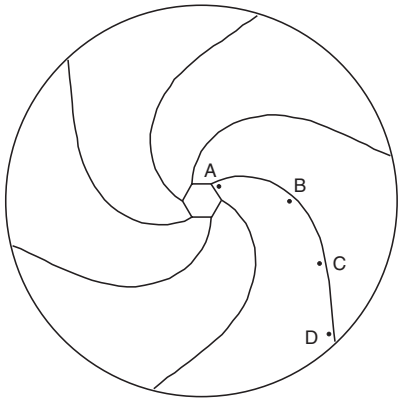

Figure 8: Cutting pattern for reflector with $D = 0.9$ m and $F/D = 0.4$.

Finally, a Vivak model was made, cut, and folded with 3 strings linking opposite petals, behind the hub. Packaged in this way, the dish could fit into a cylindrical envelope with a diameter of 0.32 m, and 0.46 m long. However, if supported from the outside the dish could be packaged more tightly, achieving a packaging ratio of 3.0.

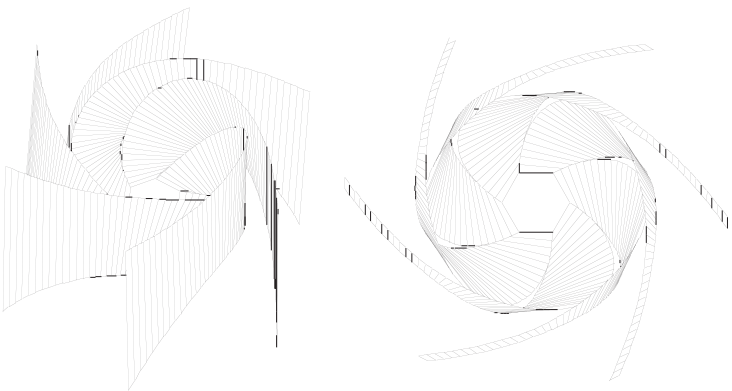

Figure 9: Views of packaged reflector.

The curvature of a petal was measured, in the packaged configuration, at the points A-D shown in Figure 8 and compared with the values that had been predicted by our simple analysis, see Table 4. At point A the expected curvature was much higher than measured, because the hub had been modelled as rigid. In practice, though, a small elastic curvature of the hub has the effect of greatly relieving the sharp curvature at the root of the petal. Elsewhere, our simple predictions are within 10% of the measured values. Note that all predictions are *conservative*.

Location	Prediction	Measurement
A	102	800
B	207	235
C	168	198
D	193	209

Table 4: Comparison of radii of curvature (mm).

6 Discussion

A new folding concept for flexible surface reflectors has been presented. The key idea is to cut the surface into 6-8 petals along lines whose shape is determined by an optimization approach that maximizes the packaging ratio of the reflector, subject to a constraint on the maximum stress.

A dish with $D = 0.9$ m and $F/D = 0.4$ has been packaged into a diameter of 0.3 m, giving a packaging ratio

of 3. This value is controlled mainly by the diameter of the transition region over which the petals are twisted through 90°. Hence, we expect that for reflectors of more realistic size more efficient packaging could be achieved, provided that the thickness of the material at the centre of the reflector can be kept small.

Practical applications of the proposed folding scheme will require a system to pull and hold together the very flexible petals. Preliminary experiments using a shape-memory alloy zipper, similar in shape to the seals that are used in plastic food bags, triggered from the hub (i.e. where the gap between the petals is smallest), has been investigated by Sutor (2002). Other important issues that remain to be addressed include the dynamic deployment behaviour of reflectors packaged according to the scheme proposed in this paper.

References

Calladine, C. R.: *Theory of Shell Structures*, CUP, Cambridge, 1983.

Guest, S. D.; Pellegrino, S.: A new concept for solid surface deployable antennas. *Acta Astronautica*, 38, (1996), 103-113.

Hibbit, Karlsson and Sorensen, Inc.: *ABAQUS/Standard User's Manual*, Version 6.2. Pawtucket, RI, USA, 2001.

Hooke, R.; Jeeves, T.A.: "Direct search" solution of numerical and statistical problems, *Journal of the Association for Computing Machinery*, 8, (1961), 212-229.

Mikulas, M. M.; Thomson, M.: State of the art and technology needs for large space structures. In: *New and projected aeronautical and space systems, design concepts, and loads*, A. K. Noor; S. L. Venneri, eds., ASME, New York, (1994), 173-238.

Robinson, S.A: Simplified spacecraft antenna reflector for stowage in confined envelopes. European Patent Application EP0534110A1, 1992.

Sutor, C.: *Zippers for deployable structures*. M.Eng Project Report, Department of Engineering, University of Cambridge, 2002.

Address: Mr B. Tibbalds, JPMorgan, 125 London Wall, London EC2Y 5AJ, U.K.
Dr S.D. Guest and Prof. S. Pellegrino, Department of Engineering, University of Cambridge, Trumpington Street, Cambridge, CB2 1PZ, U.K.
email: `ben.tibbalds@jpmorgan.com; sdg@eng.cam.ac.uk; pellegrino@eng.cam.ac.uk`